Accepted Manuscript

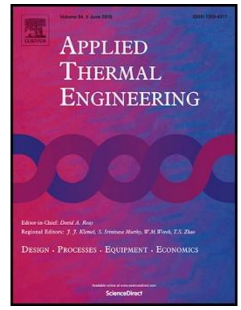

Title: Hot sanitary water production with CO_2 heat pumps: effect of control strategy ON system performance and stratification inside the storage tank

Author: M. Tammaro, A.W. Mauro, C. Montagud, J.M. Corberán, R. Mastrullo

PII: S1359-4311(16)30044-8
DOI: http://dx.doi.org/doi: 10.1016/j.applthermaleng.2016.01.094
Reference: ATE 7654

To appear in: *Applied Thermal Engineering*

Received date: 31-8-2015
Accepted date: 22-1-2016

HOT SANITARY WATER PRODUCTION WITH CO_2 HEAT PUMPS: EFFECT OF CONTROL STRATEGY ON SYSTEM PERFORMANCE AND STRATIFICATION INSIDE THE STORAGE TANK

M. Tammaro°, A. W. Mauro°#, C. Montagud *, J. M. Corberán*, R. Mastrullo°

°Dipartimento di Ingegneria Industriale, Università degli Studi di Napoli Federico II,
P. Le Tecchio, 80, Napoli, Italy. # wmauro@unina.it
* Instituto de Ingeniería Energética, Universitat Politècnica de València,
Camino de Vera s/n, 46022 Valencia, Spain.

ABSTRACT

In this work three different control strategies for the production of sanitary hot water by means of an electric heat pump working with CO_2 are investigated. The heat pump is a prototype, here modeled in the vapor-compression software package IMST-ART. By simulating this model, the performance of the heat pump is correlated to the boundary conditions and is scaled to different sizes, namely 1, 1.5, and 2 times larger than the reference system. After having chosen an application for which the load profile of sanitary hot water during the year is known, these heat pumps are simulated in a TRNSYS16 model where the production of sanitary hot water and the consumption are buffered by the presence of a tank. Key parameter in guaranteeing comfort and good performance of the system is the stratification inside the storage tank. The size of the tank necessary to keep a certain level of comfort at the user is then determined through a parametric analysis for each size of the heat pump. The energetic performance is also evaluated for each system in terms of seasonal performance factor. Then, the results obtained are compared with a different system where the heat pump is equipped with an inverter and the circulation pump follows a different control logic. The size of the tank and the seasonal performance factor are therefore determined in this case too. Moreover, a "night&day" control logic is compared to these first two options to have a baseline of comparison in terms of volume of storage needed to guarantee a same level of comfort and performance. To provide information also on the running costs a parametric analysis was run varying the type of control, the heat pump and the tank sizes for different load profiles.

The results show that the size of the heat pump has a significant effect on the comfort of the user, which usually leads to oversizing of the storage tank when the load profile is unknown. With regards to this, the results obtained for the alternative control system show a 20% reduction of the volume of the tank, given a certain level of comfort, and is therefore useful to reduce the size of the storage tank.

KEYWORDS: *storage tank control, sanitary hot water, heat pump, parametric analysis, cost.*

1. INTRODUCTION

Electrical Heat Pump (EHP) systems are of primary importance to save energy while respecting the environment, as recognized by European Regulations such as 812/2013 [1], which focuses on the evaluation of performance for sanitary hot water production by means of different technologies, such as EHP, solar and boilers. According to these recent regulations it is possible to compare different technologies on the same energetic basis, enhancing the importance of rigorous performance evaluations during the whole year. This is especially important for the EHP systems that are subject to strong variations with the weather conditions in order to evaluate appropriately the fraction of heat that could be considered as renewable. In addition to the energetic concerns the environmental issues related to the direct contribution to global warming of the most used synthetic refrigerants have pushed governments in the direction of some regulations, as the F-gas in Europe, that limits the use of current fluorinate refrigerants. New synthetic refrigerants or natural ones can fit the new restrictions.

The use of low environmental impact fluids, like CO_2, could be particularly advantageous if their use as a refrigerant brings to performances which are even better than those of HFC systems. In particular, the use of CO_2 heat pumps has been proved to be efficient, in comparison to HFC systems, for the production of hot sanitary water with large temperature lift, especially when the temperature of the water to the user/storage tank is over 60 °C starting from the value of the water supply network.

Several studies have been carried out focusing on the design of the EHP system and some best practices are commonly used for some reference conditions. For example, the adoption of carbon dioxide (CO_2) has been proposed in by Rieberer et al. (1997) [2] and by Neksa et al. (1998) [3]; also the advantage of its use has been proved, with respect to standard solutions, by Cecchinato et al. (2005) [4].

More recently, as shown in Zhang et al. [5], CO_2 heat pumps have become a standard solution for the production of sanitary hot water in some markets, such as the residential market in Japan, where electricity has been historically favoured in comparison with natural gas as source of energy. Optimization of the performance with a CO_2 heat pump for sanitary water requires controlling the gas cooler pressure, as the thermodynamic cycle is usually transcritical (Lorentzen, [6]). This is shown in works, such as Cecchinato et al. [7] and Kauf [8], where some functions are suggested to control the gas cooler pressure in order to maximize the COP as a function of the boundary conditions, such as ambient temperature (Yokoyama et al. [9]) and water inlet temperature (Qi et al. [10]). EHPs for the production of sanitary hot water are usually coupled to storage tanks in order to separate the process of water heating (whose duration is influenced by the necessity of operating the compressor at least for some minutes to avoid breakage) from the consumption (which can last for seconds); the sanitary hot water is therefore taken from the storage tank, which is refilled with water from the supply network, ready to be heated in the gas cooler of the EHP. For this reason, water inlet temperature at the gas cooler of the CO_2 heat pump is a function of the temperature distribution inside the tank.

Studies such as Castell et al. [11] show the parameters affecting the stratification of temperatures inside the tank and the way to characterize it. In particular, the authors indicated a height-to-diameter ratio of 3-4 to better preserve stratification along the height of the tank. In Fernandez-Seara et al. [12] it is shown how the amount of hot water demanded affects stratification inside the tank and how the control logic of the heating system affects the temperature of delivery to the user. In Fernandez et al. [13] the authors show that a better stratification inside the tank induces lower water inlet temperatures at the gas cooler of the EHP, which affects the COP positively. Therefore the authors show that reheating water after standby losses is a process with a 30-40% lower COP than heating cold water from the supply network. In Yokoyama et al. [14] the effect of the variation of the amount of hot water consumed by the user on the performance of a CO_2 EHP is evaluated. The authors quantified the influence of the demand of hot water on the distribution of temperature and the amount of hot water stored inside the tank. In terms of energetic performance of the system, given a control logic which turned OFF the heat pump when water reached 30 °C at the bottom of the tank, they did not find a large impact of the demand on the COP.

Therefore, depending on the load profile, the size of the storage and its control logic could have a large effect on the performance of the EHP coupled to the user and on the temperature of delivery to the user. The estimation of the performance impact of the adoption of different control logics on the energy performance of EHPs is part of an ongoing FP7 European Project, Next Generation of Heat Pumps working with Natural fluids, NxtHPG (Corberan & Montagud, [15]).

In this paper the results of the seasonal performance evaluation for a CO_2 EHP, coupled to a stratified storage tank and a real user profile are presented. Firstly, it is evaluated the volume of the storage size required to reach a certain delivery temperature to the user given a certain size of the heat pump and a control logic. Then, three control logics are compared from an energetic point of view for different sizes and for different types of user demand profiles. Finally, a running costs analysis connected to the different control logics is carried out.

2. HEAT PUMP MODELLING: PERFORMANCE CORRELATIONS

The EHP (reference case) is an air-to-water model working with CO_2 (R744). Its nominal heating capacity $\dot{Q}_{gc,nom}$ is of 29.4 kW when heating a nominal flow rate $\dot{m}_{gc,nom}$ of 506 kg/h of water from $T_{in,gc}$ 10 to $T_{out,gc}$ 60°C at the gas cooler at an ambient temperature T_{amb} of 7°C. In these conditions, the nominal Coefficient of Performance (COP) COP_{nom} is 3.95.

Its main characteristics are:

- Compressor: reciprocating, semi-hermetic, 64.5 cm^3 displacement at 50 Hz;
- Evaporator: tubes and fins heat exchanger, 77 m^2 external surface;
- Gas cooler: plates, UA 3700 W/K.

The EHP is modelled in the vapour-compression software package IMST-ART. IMST-ART (Corberan & Gonzalvez, [16]). is able to calculate the evolution of the refrigerant throughout all the components of the system. It employs a fine discretization of the HEs following a special numerical technique to provide high accuracy in the integration as well as short computation time and high numerical robustness (Corberan et al. [17]).The evaluation of the void fraction, thermodynamic properties as well as friction and heat transfer is local.

By simulating the model, which determines the optimal gas cooler pressure for each set of conditions, a map of performance is obtained as a function of ambient temperature, water inlet temperature and mass flow rate at the gas cooler, so that the heating capacity $\dot{Q}_{gc}$, in kW, and other performance indicators are correlated as shown in Eq. (1):

$$f(x,y,z) = p_1 + p_2 x + p_3 y + p_4 z \quad (1)$$

where x is the ambient temperature T_{amb} in °C, y is the water inlet temperature at the gas cooler in °C $T_{in,gc}$, z is the water flow rate at the gas cooler, $\dot{m}_{gc}$, in kg/h. Table 1 reports the values of the coefficients p_n obtained for the main performance indicators, whereas Figs. 1 and 2 show the performance maps obtained by fitting data: as an example, here $\dot{m}_{gc}$ is fixed to the value such that the water outlet temperature at the gas cooler $T_{out,gc}$ = 60 °C for each couple of (T_{amb}, $T_{in,gc}$).

In Fig.1 it is shown how the heating capacity increases with the ambient temperature and decreases slightly with the water temperature at the inlet of the condenser, while in Fig.2 it is shown how the electric power increases with the latter: in Fig. 3 the COP of the EHP is shown: it increases with the ambient temperature and decreases with the water inlet temperature. The values calculated by the correlations have a <10% mean absolute percentage error (MAPE) with regards to the experimental values measured on the prototype.

Since this paper focuses on different control options for the system, including the presence of an inverter coupled to the compressor, the extensive parameters of the ON/OFF EHP just shown are used as a baseline reference (*ref*) and are scaled, as shown in Table 2, in order to model different sizes of the heat pump (1.5 times and 2 times as large) and the presence of an inverter of a compressor. In the same table the intervals considered for the three boundary conditions are indicated.

$\dot{V}_{comp}$, A_{gc}, A_{ev}, $\dot{V}_{fan}$ are respectively: swept volume of the compressor, gas cooler heat transfer area, evaporator heat transfer area and volumetric flow rate of the fan.

By doubling the area of the heat exchangers and the volumetric flow rate at the compressor and at the fan, the thermodynamic cycle of the refrigerant remains similar to the starting one while the heating capacity is close to doubled. This allows to investigate the effect of the size of the heat pump on the interaction with the tank and, therefore, with the user demand, by means of a parametric analysis.

2ref and *inv* model a heat pump twice as big as the reference case one in terms of heat exchangers; the former has the compressor scaled up as well, while the latter works with the same size of compressor used in the *ref* case. Therefore, *2ref* and *inv* will be used to model the performance of a heat pump with an inverter compressor working at 60 and 30 Hz respectively. Performance at all other frequencies is obtained by interpolating linearly between these two. Across all sets of correlations, the mean absolute percentage error (MAPE) is < 3% for the heating capacity, < 10% for the compressor power and <8% for the COP (comparison of the value calculated by the correlations and the value simulated by the model).

3. END USERS DESCRIPTION

To assess the influence of the heat pump size and the storage on the discomfort, the case study of an educational building and is considered. A weekly load profile is reported, per person, in Fig.4, taken from Koiv et al. [18]. The educational building load profile is scaled so that the average heating load matches the capacity of the heat pump of the reference size *ref* working at an ambient temperature of -2 °C and a water inlet temperature at the gas cooler of 10 °C. This leads to a scale factor of 350 (people), equal to an average heating capacity of 26 kW.

To compare the control logics, in the second part of the results, the educational building load profile was rescaled to 250 people (equal to an average power of 19 kW). Moreover, a hospital load was considered. This was obtained experimentally and is shown in Fig. 5. The hospital load profile is scaled in such a way that the average heating load is two times the educational building load (38 kW). Therefore, a scaling factor of 9 (units) is considered in this case.

In all cases the location of the end users is Strasbourg, France, which is the average climate of Europe according to [1].

The hot water consumption also varies with the monthly average temperature in the chosen location, in such a way that during every day of the coldest month of the year an extra 20% of water is consumed and in every day of the warmest month 20% less hot water is consumed. This reflects the fact that during warmer seasons less hot water is consumed and at a slightly lower temperature (Energy Saving Trust, [19]).

4. SYSTEM MODEL

A model in TRNSYS was developed in order to perform transient simulations of the systems. The schematic of the system in the *reference case* is that presented in Fig. 7. The air-to-water EHP is used to produce SHW at 60 °C. This temperature is obtained by means of an inverter control (20 - 50 Hz) on the circulation pump, which modulates the water flow rate according to the EHP boundary conditions (ambient temperature and water inlet temperature at the gas cooler). The compressor is an ON/OFF type; its cycles are controlled by the temperature measured at a certain point in the tank T_{set} and a deadband db so that a certain volume of hot water is always available for the user to withdraw. The same schematic and control logic applies to the *night&day* cases which will be introduced later. A different control, named *inverter case*, is presented in Fig. 8. Here $T_{out,gc}$ is controlled by means of an inverter (30 - 60 Hz) coupled to the compressor, while the circulation pump varies its speed (20 - 50 Hz) in order to maintain constant temperature in the middle of the tank. In theory, in fact, if $\dot{m}_{gc}$ and $\dot{m}_{tank}$ were equal at all times, a complete stratification inside the tank would be maintained. By following the variation of temperature in a certain point of the tank and trying to keep it to zero, this control tries to obtain a complete stratification. If this is possible, then a smaller tank can be adopted without increasing the discomfort of the user. A deadband of 5 K is still present, so that the heat pump turns OFF when the temperature in the middle of the tank exceeds a certain value named T_{set} which is equal to 45 °C and then back ON when the temperature is lower than T_{set} minus db .A schematic of the tank with the set temperature and the deadband is reported in Fig.6.

In all systems, water is delivered to the user at 50 °C (T_{user}) by means of a tempering valve although any value between 40 °C and 50 °C is acceptable. This considers the fact that different usages of SHW require different temperatures (ASHRAE Handbook, [20]). The storage tank has a height-over-diameter ratio equal to 4 in order to help maintain stratification, is well insulated and kept in a close environment at a constant 20 °C. It is modeled as one dimensional and water entering from the top and bottom is fully mixed, split into nodes of equal volume (Type 60c in the TRNSYS16 library). On each i-th node a mass balance and the energy balance of Eq. (2a) are solved.

$$M_i c_{p,f} \frac{dT}{d\theta} = \alpha_i \dot{m}_H c_{p,f} (T_H - T_i) + \beta_i \dot{m}_L c_{p,f} (T_L - T_i) + UA_i (T_{amb} - T_i) + F \qquad \text{(2a)}$$

In Eq. (2a) α is 1 if the i-th node considered is the top of the tank and 0 otherwise; β is 1 if the i-th node considered is the bottom of the tank and 0 otherwise; T_H and T_L are the temperatures of hot water entering from the top and cold water entering from the bottom, respectively; F is a factor shown in Eq. (2b).

$$F = \gamma_i c_{p,f} (t_{i-1} - t_i) \text{ if } \gamma_i > 0;\; F = \gamma_i c_{p,f} (t_i - t_{i+1}) \text{ if } \gamma_i < 0 \qquad \text{(2b)}$$

The coefficient γ is defined in Eq. (2c), where N refers to the number of nodes in the tank.

$$\gamma_i = \dot{m}_H \sum_{j=1}^{i-1} \alpha_j - \dot{m}_L \sum_{j=i+1}^{N} \beta_j \qquad \text{(2c)}$$

Reintegration water from the supply network has a constant temperature of 10 °C. The model works in quasi-steady state, simulations are run during a year (8760 hours) and the time step is of 1 minute.

5. RESULTS: USER DISCOMFORT VS. STORAGE SIZE

A first parametric analysis is conducted for the layout depicted in Fig. 7 and three different sizes of heat pumps, namely *ref*, *1.5ref*, *2ref* (refer to Table 2) with the educational building load profile. The purpose is to evaluate performance of the system in terms of SPF1, defined as in Eq. (3) and to determine the size storage needed to remain below a certain level of discomfort of the user.

$$SPF1 = \frac{\int_0^{8760} \dot{Q}_{gc}\, dt}{\int_0^{8760} \dot{L}_{comp}\, dt} \qquad (3)$$

The level of discomfort is measured by the percentage of water delivered to the user at a temperature lower than 40 °C, as shown in Eq. (4).

$$\% \dot{m}_{discomfort} = 100 \cdot \frac{\int_0^{8760} \dot{m}_{Tuser<40} dt}{\int_0^{8760} \dot{m}_{user} dt} \tag{4}$$

Moreover, the percentage of ON time of the compressor is reported, defined as in Eq. (5).

$$\% ON = \frac{\sum_1^N \int_{t_{start}}^{t_{end}} dt}{\int_0^{8760} dt} \tag{5}$$

In Table 3 the input data the simulation parameters are summarized. The percentage of "hot" volume $\% V_{hot}$ is the volume above the height where the temperature is measured in the tank. So for example, a $\% V_{hot}$ equal to 50 means that the temperature is measured at the middle of the height of the tank and therefore the upper half of the tank's volume is filled with hot water at all times.In fact, given that the set temperature T_{set} is 45 °C and that the deadband db is 5 K, this volume is always at a temperature higher than 40 °C (minimum acceptable temperature for the water to be considered hot, as previously stated). The results of the simulations are summarized in Table 4.

In all cases, it can be seen how the discomfort decreases when the volume of the tank increases. Absolute values of the volume of the tank needed for a similar level of discomfort decrease with the increase of the size of the heat pump. The SPF seems to be largely unaffected by the choice of the volume of the tank, given the heat pump: this is due to the fact that $\% V_{hot}$ is 50% in all cases: this means that the other 50% of the tank is large enough to maintain a good stratification inside.

In Fig. 9 the discomfort results are reported as a function of the volume of the tank. It is shown how the matching of the heat pump capacity and the size of the storage significantly affects discomfort. By setting the maximum allowable level of discomfort to 5%, it is possible to determine the tank volume needed for the application. In particular, as $\% V_{hot}$ is 50% of the total in these simulations, it is possible to determine how much water needs to be stored at high temperature. For the heat pump sizes considered (*ref*, *1.5ref*, *2ref*), these values are: 7200, 4000, 1200liters of total volume of the tank respectively, which mean 3600, 2000, 600liters of hot water stored at all times with the given control logic.

6. RESULTS: CONTROL LOGIC COMPARISON

Two different type of control of the systems are now considered. The first one is illustrated in Fig. 8. In this system, the heat pump is the *2ref* size with an inverter controller that reduces frequency from 60 down to a minimum value of 30 Hz. As previously explained, in this layout (named “inverter case”) the circulation pump feeding the gas cooler is equipped with an inverter which tries to maintain a constant temperature inside the tank. The second one is a system equal to that of the reference case (Fig. 7) with a different control logic, a so-called “night&day” logic. According to the “night&day” logic, it is best to keep the heat pump running during the night only to take advantage of the lower electricity prices which are offered in some countries of Europe. In order to do so, the heat pump is forced to be OFF during the day (from 8 to 20h in this study) and a much larger tank is adopted so that enough hot water can be stored during the night (from 20 to 8h). Taking into consideration the educational building profile located in Strasbourg, the reference case and the “night&day” case are simulated with three heat pump sizes *ref, 1.5ref, 2ref,* while the inverter case is simulated with the *2ref-inv* heat pump, as previously explained. Inputs are summarized in Table 5. Please note that the volume of the tank shown among the results in Table 6 was chosen for each case with a parametric analysis in order to guarantee a discomfort close to 5%. Therefore discomfort will not be shown among the results from now on.

Other than the parameters introduced earlier, the average duration of an ON phase of the compressor, named *adc* (average duty cycle, in hours) and defined as in Eq. (6) will be considered.

$$adc = \frac{1}{N}\sum_{1}^{N}\int_{t_{start}}^{t_{end}} dt \tag{6}$$

Also, the average temperature on the bottom of the tank during ON phases, defined as in Eq. (7), will be considered, being it a measure of the effectiveness of the stratification inside the tank.

$$T_{bottom,avg} = \frac{\sum_{1}^{N} \int_{t_{start}}^{t_{end}} T_{bottom}\, dt}{\sum_{1}^{N} \int_{t_{start}}^{t_{end}} dt} \tag{7}$$

Moreover, the consumption of the compressor will be split into day and night consumption, in order to evaluate running costs given an electricity price scenario later. Results are summarized in Table 6.

From the results it can be noted how the compressor consumption is concentrated mostly during the day, when there is demand of hot water, except in the “night&day” cases, where the heat pump is kept on OFF during the day and works during the night. In all cases, including the “night&day” ones, the $\%V_{hot}$ was chosen to be 80% with the remaining 20% was dedicated to stratification towards the bottom of the tank. The values of the average temperatures on the bottom of the tank $T_{bottom,avg}$ remain below 23 °C in all cases, indicating good stratification. This contributes to maintain limited differences between the SPF among the different cases. Average compressor running times *adc*shows significant difference between the cases: the larger the heat pump size, the shorter the duty cycles. With regards to this, the inverter case control shows a beneficial effect: if compared to the reference case with the *2ref* size heat pump, in fact, it can be seen in Table 6 how the *adc* is of 1.06 hour instead of 0.16 hours, which contributes to a longer compressor life; if compared to the reference case with the *1.5ref* size heat pump, it can be seen, instead, that while energetic performance is very similar, the volume of the tank is about 2/3 smaller. Also, it can be noted how the “night&day”cases require much larger storage tanks than the other cases. Increasing the size of the heat pump with this control logic does not bring the same storage volume reduction as with the reference control logic. In the “night&day” logic, in fact, the storage volume is affected first and foremost by the amount of hot water required by the user, given that the heat pump is not allowed to catch up with the demand during the day. The *2ref-inv* case needs the smallest volume among the cases considered.

In Figure 10 a) and b) one day of simulation is shown for the *2ref* system with the reference case control logic. In Figure 11 a) and b) the same day of simulation is shown for the system with inverter*2ref-inv*.

An ON/OFF cycle of the EHP can be seen from the heating capacity in Fig. 10b from 7 to 8h, when the heating capacity drops again to 0. *T deliv SHW* is the temperature of water withdrawn by the user: during the first draw-off of the day, water at around 30 °C is extracted (point A); this is due to the heat losses along the distribution circuit during the night. Temperature at the bottom of the tank *T bottom*, in green, is at around 25 °C at the beginning of the day (point B): the stratification is lost because the share of volume below the control position (20%) is not large enough to keep the bottom close to the temperature of the supply network (10 °C) in this moment. In Fig. 9b it can be noted how the mass flow rate of water heated by the EHP, in green, is higher than the one extracted by the user, *Showers* in red, except at around 11 and 13 hours (points C and D). The mismatch between the flow rates causes the ON/OFF working cycles to be quite frequent and brief (15 cycles from 7 to 22h).

In Fig. 11a it can be seen how the *T Control* oscillates between 40 and 50 °C from 7 to almost 8h: this is an ON/OFF cycle of the EHP, as it can be seen from the heating capacity in Fig. 11b at the same hours (point E). *T deliv SHW* remains above the acceptable temperature threshold (40 °C) as in the previous case. In this case the temperature at the bottom of the tank *T bottom*, in green, is at around 15 °C at the beginning of the day (point F): the stratification is better preserved thanks to the inverter control in this case. Also, the longer ON cycles are such that stratification is maintained during the day, as it can be noted for example between 11 and 16h in Fig. 11b. Between 11 and 16h in the reference case (Fig. 10b, point G), instead, stratification is lost and *T Control*drops to the level of the bottom. In Fig. 11b it can also be noted how the mass flow rate of water heated by the EHP is similar to the one extracted by the user, except when demand is low. The smaller mismatch between the flow rates, result of the control system, coupled to the presence of the inverter on the compressor, causes the ON/OFF working cycles to be longer and less frequent (6 cycles from 7 to 22h). The peaks of flow rate at the beginning of each cycle are due to imperfect calibration of the PID controller of the circulation pump.

The comparison between the control logics is now carried out for the hospital load profile. As previously stated, this load profile is scaled up to be twice as large as the educational building load profile, in terms of average heating capacity required to meet the user needs of SHW. The inputs for the simulations are reported in Table 7. The night&day cases are marked here with an asterisk (*). This is because it was impossible to reach the 5% discomfort objective by adopting a strict night&day logic with the three heat pump sizes chosen for the comparison: even with the *2ref* size, the heat pump could not heat up a sufficient amount of water working only during the twelve hours (20 – 8h) of the night, whereas with the other control logics the *2ref* size of the heat pump turned out to be large enough to meet the objective. For this reason, the "night&day" control logic here was partially modified: the heat pump could turn ON during the day until 20% of the volume was filled with hot water (and could work during the night to fill 80% of the volume as usual). This modified "night&day" control logic can therefore be considered as a hybrid with the reference logic and the volume of the tank reached with the *2ref* heat pump is in fact quite similar between the two control logics, as it can be seen in Table 8. The distribution of electrical consumption between night and day is also now shifted towards the day, especially when the *2ref*size heat pump is considered. However, the *2ref-inv* control logic requires a smaller volume for this user type too.

Next, a running costs comparison is carried out for the two user types between the control logics. As it can be seen in the statistics concerning Europe, such as [21], the internal market in Europe is composed of a mix of regulated and free markets. Taking into account differences into taxation and subsidization between the countries too, it emerges that prices vary notably from place to place and with the size of the consumer considered. Moreover, in some places it is possible that during the night (20 to 8h in this work) electricity prices are remarkably lower than during the day. For this reason, instead of choosing one value for the electricity price at night and one for the day, running costs will be normalized with regards to the highest calculated running cost for each user type, while the night and day electricity difference in price (per kWh) will be taken into account through their ratio. In Eq. (7) the ratio between night and day electricity prices is reported.

$$P_{ratio} = \frac{\mathrm{Price}_{night}}{\mathrm{Price}_{day}} \tag{7}$$

The normalized running costs RC for each case considered (“actual” case) are normalized to a “reference” case (i.e. the highest calculated running cost for each user type). This is expressed in Eq. (8a).

$$RC = \frac{Cost^{actual}}{Cost^{reference}} = \frac{L^{actual}_{comp,day} \cdot \mathrm{Price}^{actual}_{day} + L^{actual}_{comp,night} \cdot \mathrm{Price}^{actual}_{night}}{L^{reference}_{comp,day} \cdot \mathrm{Price}^{reference}_{day} + L^{reference}_{comp,night} \cdot \mathrm{Price}^{reference}_{night}} \tag{8a}$$

This is equal to Eq. (8b):

$$RC = \frac{L^{actual}_{comp,day} + L^{actual}_{comp,night} \cdot P^{actual}_{ratio}}{L^{reference}_{comp,day} + L^{reference}_{comp,night}} \tag{8b}$$

given that $\mathrm{Price}^{actual}_{day} = \mathrm{Price}^{refrerence}_{day}$ and $P^{reference}_{ratio} = 1$.

The distribution of consumption between night and day is summarized for all cases in Fig. 12, while the running costs results are shown in Fig. 13 and 14 respectively for the educational building and hospital load profiles. Fig.13 shows that the reference cases running costs are marginally impacted by the cost of electricity at night and so is the *2ref-inv* case, which is almost overlapped to the *1.5ref* case. This is due to the fact that the SHW demand is concentrated mostly during the day for this user type and so is the electrical consumption. Both for the reference control logic and for the “night&day” one, an increase in size of the heat pump causes an increase of the running costs. The “night&day” cases show lower running costs than the reference cases up to a value of around 0.93 of the P_{ratio}. The reduction in running costs needs to be compared against the cost of the larger storages which are needed.

Fig. 14 shows different trends within each control logic, due to the demand profile being more evenly spread between day and night for the hospital case. For the reference case control logic, in fact, the larger heat pump (*2ref*) causes electrical consumption to be prevalent during the day, while the smaller heat pump (*ref*) has 50% of the consumption during the day (as shown in Table 8) and therefore is more positively affected by a reduction in price of the electricity during the night. It can also be observed that, given the modified "night&day" logic, in the hospital case the size of the heat pump has an impact on the distribution of the consumption (and therefore of the costs) between night and day. Within the modified "night&day" cases we find both the one with the highest running costs (*2ref* heat pump size) and the one with the lowest running costs (*ref* heat pump size) regardless of the P_{ratio}. The former is also the case with the lowest SPF, which causes a larger consumption, and with the highest consumption during the day. The latter, instead, has the largest night consumption among all cases. The inverter case consumption distribution causes it to perform best when no difference in price between night and day is present (P_{ratio} = 1) and similarly to the *1.5ref* case when P_{ratio} tends to zero. The running costs for the inverter case, however, need to be considered together with the costs of a smaller storage and with the cost of the extra inverter coupled to the compressor, not present in any of the other cases.

6. CONCLUSIONS

The effect of the control strategy on the performance of a sanitary hot water production system based on a CO_2 electric heat pump was presented for two user types. The heat pump performance was correlated to its boundary conditions and was scaled to different sizes to investigate its matching with the storage size, given a control logic and a certain user load profile.

In general, it was shown that larger heat pumps and larger storage tanks correspond to less discomfort of the user.

In particular, fixed a 5% discomfort level to have a common basis of comparison for this important constraint for the user, the results showed that a twice as large heat pump corresponded to a 6 times smaller tank. In terms of energetic performance, the seasonal performance factor was not affected heavily by the size of the tank in a large range of sizes, given the control strategy adopted which allowed to maintain a good stratification.

Then, different types of control of the system were examined, keeping the discomfort at 5%, since they affect the size of the tanks, the energetic performance and the distribution of the energy consumption among the day and the night (i.e., the running costs). The types of control are three: a reference one, a new one with inverter controls and a basic “night&day” control logic.

The “night&day” control logic proved to be economically more advantageous in combination with the smallest heat pump, although it needed a very large storage not to induce discomfort to the user (up to 30 times larger, with larger plant costs).

The proposed control logic based on the inverter, where stratification in the tank is maintained over a large range of variation of demand on the user side is useful in situations where the load profile of the user is unknown, as is almost always the case. In fact, without the inverter on the compressor, matching of the heat pump size and the tank affects discomfort considerably, which leads – usually – to oversizing the tank to avoid discomfort.

The proposed control logic slightly reduces electrical consumption and it needs a much smaller tank than the most economically convenient “night&day” case (up to 10 times smaller). In terms of running costs, it is not competitive if electricity prices vary between day and night and if the demand is mostly concentrated during the day.

ACKNOWLEDGMENTS

The study related to this work has been partially supported by the FP7 European project ‘Next Generation of Heat Pumps working with Natural fluids’ (NxtHPG).

The work of M. Tammaro on electric heat pumps is financially supported by Università degli Studi di Napoli Federico II throughthe FP7 European project ‘Next Generation of Heat Pumps working with Natural fluids’ (NxtHPG).

REFERENCES

[1] European Regulation (EU) 812/2013, available at: http:/eur-lex.europa.eu

[2] Rieberer R, Kasper G, Halozan J, CO2–a chance for once through heat pump heaters, CO2 technology in refrigeration, heat pumps and air conditioning systems, 1997, IEA Heat Pump Centre, Trondheim, Norway..

[3] Nekså P, Rekstad H, Zakeri G R, Schiefloe P A, CO_2 – heat pump water heater: characteristics, system design and experimental results, Int. J. Refrigeration, vol. 21(3), 1998: 172-179.

[4] L. Cecchinato, M. Corradi, E. Fornasieri, L. Zamboni. Carbon dioxide as refrigerant for tap water heat pumps: A comparison with the traditional solution. International Journal of Refrigeration 28 (2005): 1250-1258.

[5] Zhang J-F., Qin Y., Wang C-C. Review on CO2 heat pump water heater for residential use in Japan. Renewable and Sustainable Energy Reviews, Volume 50, October 2015, Pages 1383-1391.

[6] G. Lorentzen. Revival of carbon dioxide as a refrigerant. International Journal of Refrigeration, 17 (5) (1994), pp. 292–300.

[7] L. Cecchinato, M. Corradi, S. Minetto. A critical approach to the determination of optimal heat rejection pressure in transcritical systems. Appl Therm Eng, 30 (2010), pp. 1812–1823.

[8] F. Kauf. Determination of the optimum high pressure for transcritical CO_2 refrigeration cycles. Int J Therm Sci, 38 (4) (1999), pp. 325–330.

[9] R. Yokoyama, T. Shimizu, K. Ito, K. Takemura . Influence of ambient temperatures on performance of a CO2 heat pump water heating system. Energy, 32 (2007), pp. 388–398.

[10] P.-C. Qi, Y.-L. He, X.-L. Wang, X.-Z. Meng. Experimental investigation of the optimal heat rejection pressure for a transcritical CO_2 heat pump water heater. Appl Therm Eng, 56 (2013), pp. 120–125.

[11] A. Castell, M. Medrano, C. Solé, L.F. Cabeza. Dimensionless numbers used to characterize stratification in water tanks for discharging at low flow rates. Renewable Energy, Volume 35, Issue 10, October 2010, Pages 2192-2199.

[12] José Fernández-Seara, Francisco J. Uhía, Ángel Á. Pardiñas, Santiago Bastos. Experimental analysis of an on demand external domestic hot water production system using four control strategies. Applied Energy, Volume 103, March 2013, Pages 85-96.

[13] Nicholas Fernandez, Yunho Hwang, Reinhard Radermacher. Comparison of CO2 heat pump water heater performance with baseline cycle and two high COP cycles. International Journal of Refrigeration, Volume 33, Issue 3, May 2010, Pages 635-644

[14] Ryohei Yokoyama, Tetsuya Wakui, Junya Kamakari, Kazuhisa Takemura. Performance analysis of a CO2 heat pump water heating system under a daily change in a standardized demand. Energy, Volume 35, Issue 2, February 2010, Pages 718-728.

[15] Corberan J.M., Montagud C., Project NxtHPG: Next Generation of Heat Pumps working with natural fluids. 11th IIR Gustav Lorentzen Conference on Natural Refrigerants, Hangzhou, China. 2014. Conference Proceedings: ID 79.

[16] Corberan J.M., Gonzalvez J. "ART", a computer code to assist the design of refrigeration and A/C equipment, Proc. of 2002 Purdue Refrigeration Conference, West Lafayette, Indiana, USA., 94 – 95, 2002.

[17] Corberan, J. M., de Cordoba P. F., Gonzalvez J., and Alias F. Semiexplicit method for wall temperature linked equations (SEWTLE): A general finite-volume technique for the calculation of complex heat exchangers. Numerical Heat Transfer Part B-Fundamentals 40 (1): 37-59, 2001.

[18] Teet-Andrus Koiv, Alo Mikola, Alvar Toode. DHW Design Flow Rates and Consumption Profiles in Educational, Office Buildings and Shopping Centres. Smart Grid and Renewable Energy, 2013, volume 4, 287-296.

[19] Energy Saving Trust. Measurements of Domestic Hot Water Consumption in Dwellings, 2008.

[20] ASHRAE Handbook HVAC Applications, 2007.

[21] Eurostat. Energy price statistics, updated on May 2015, available at http://ec.europa.eu/eurostat/statistics-explained/index.php/Energy_price_statistics

FIGURES WITH CAPTIONS

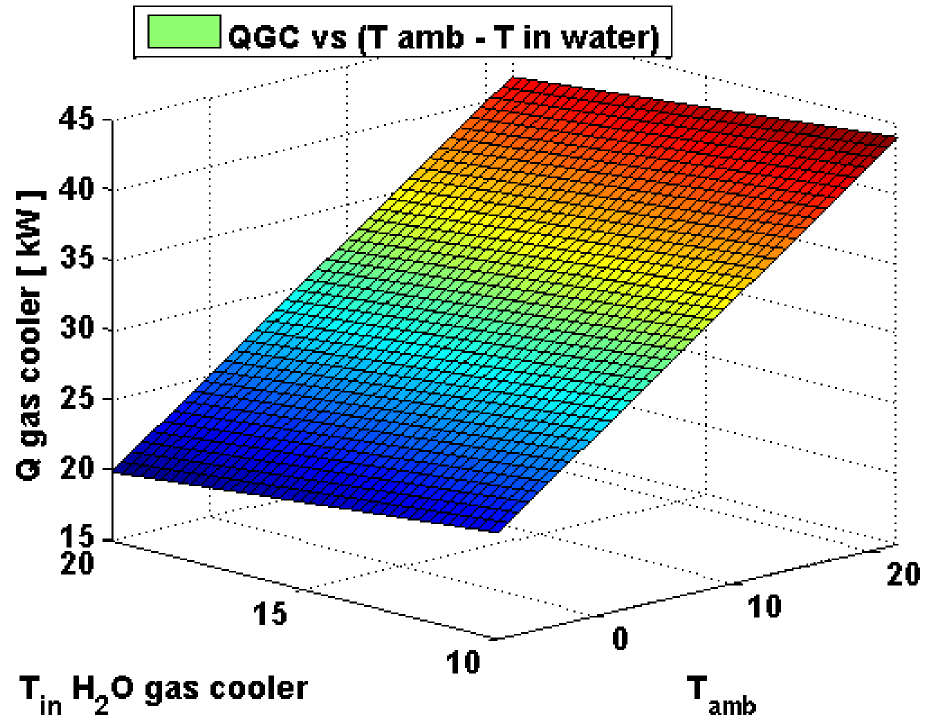

Figure 1. Heating Capacity of the EHP as a function of ambient and water inlet temperatures.

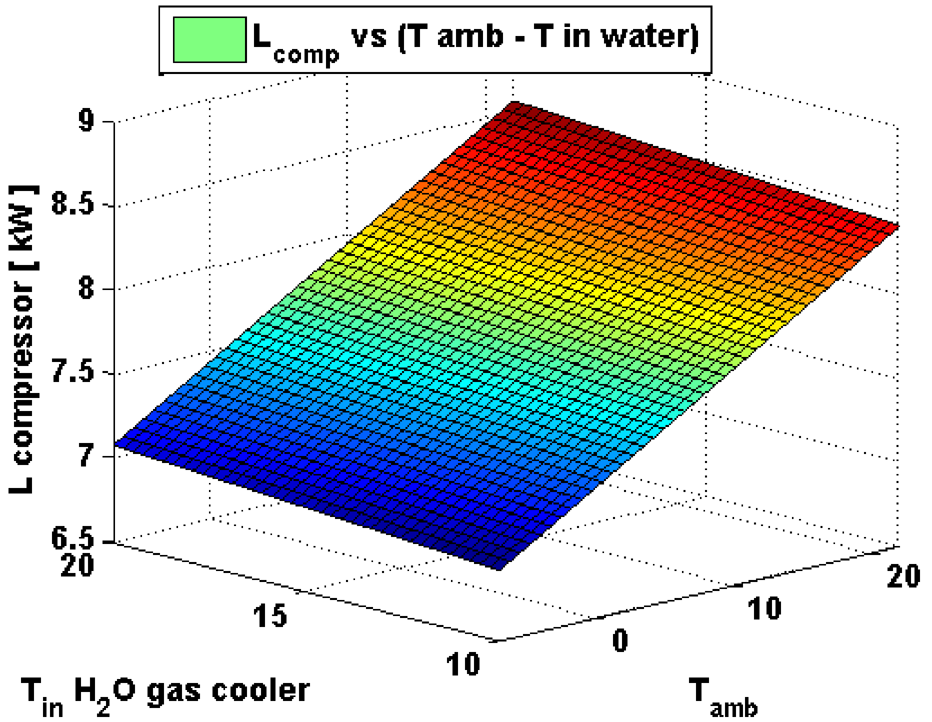

Figure 2. Compressor power of the EHP as a function of ambient and water inlet temperatures.

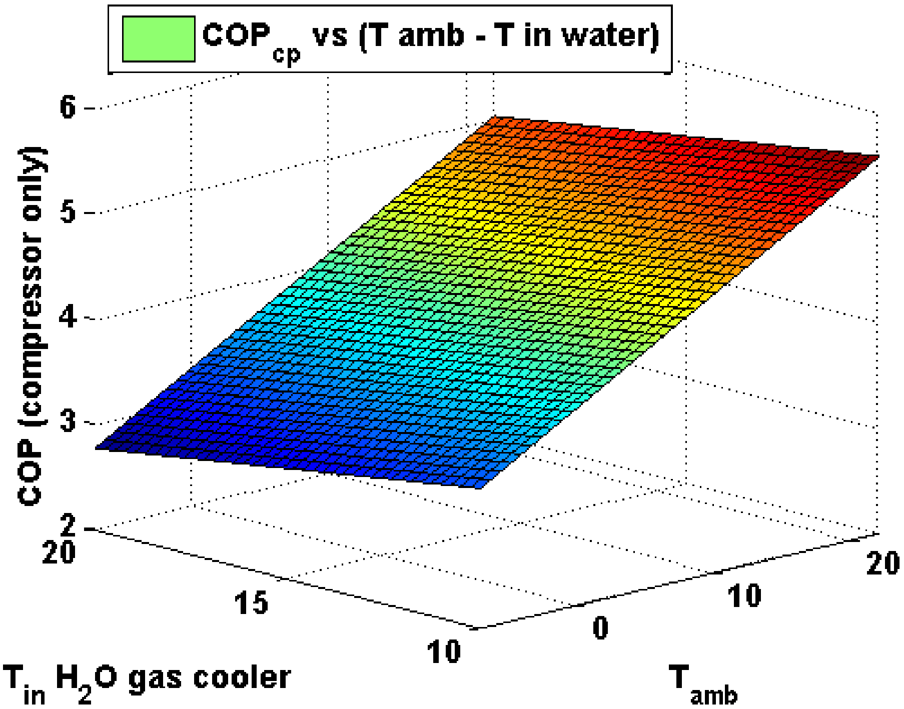

Figure 3. COP of the EHP as a function of ambient and water inlet temperatures.

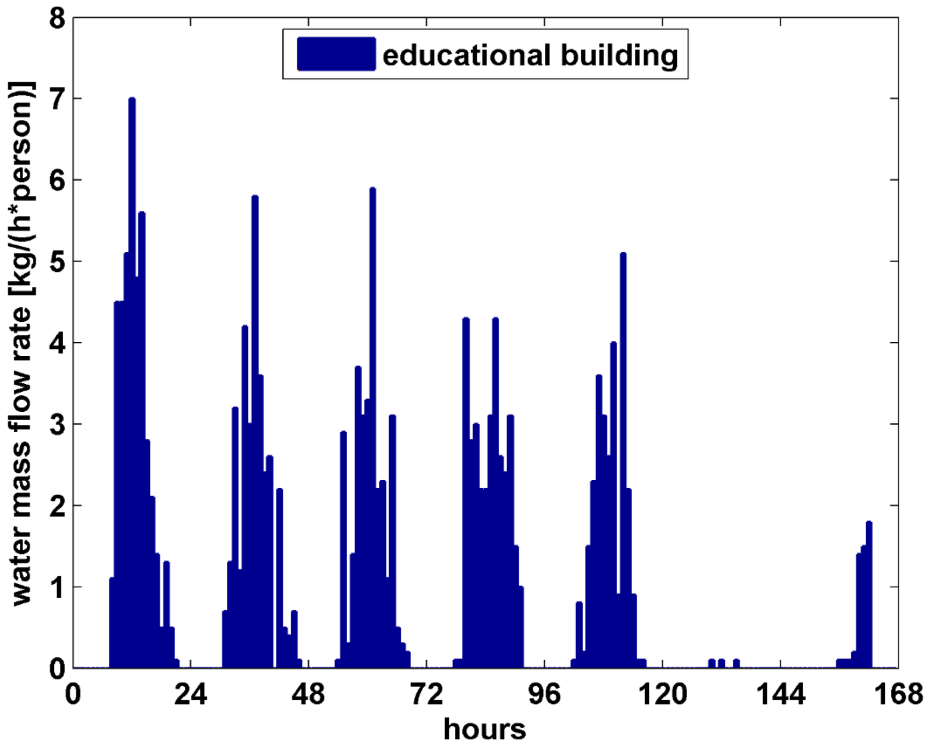

Figure 4. Educational building load profile, per person.

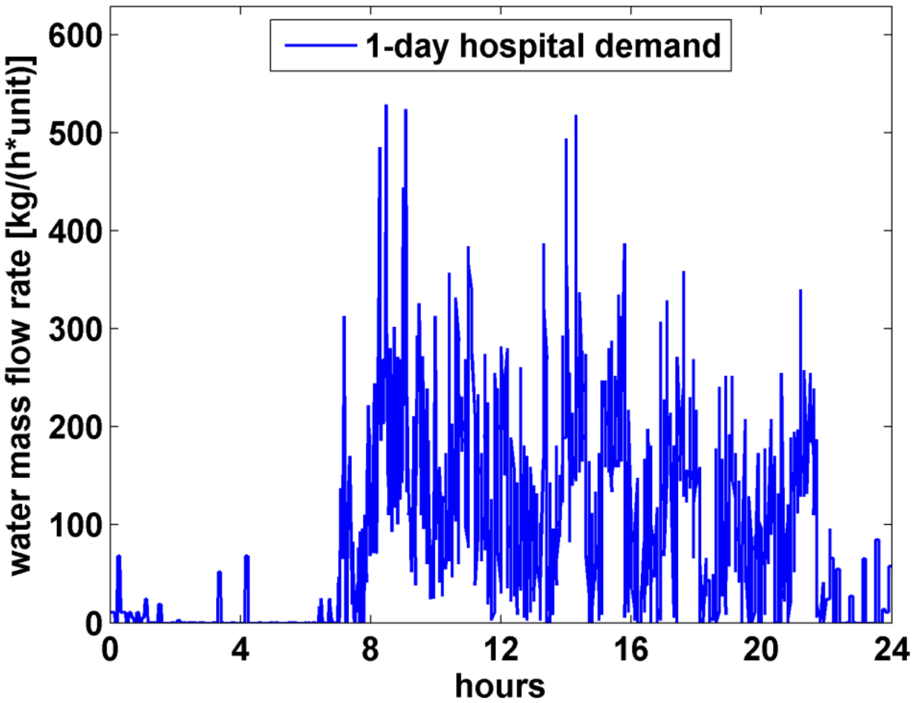

Figure 5. Hospital load profile, per unit.

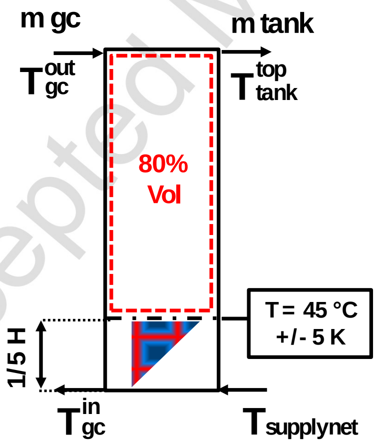

Figure 6. Schematic of the tank with the set point and the deadband.

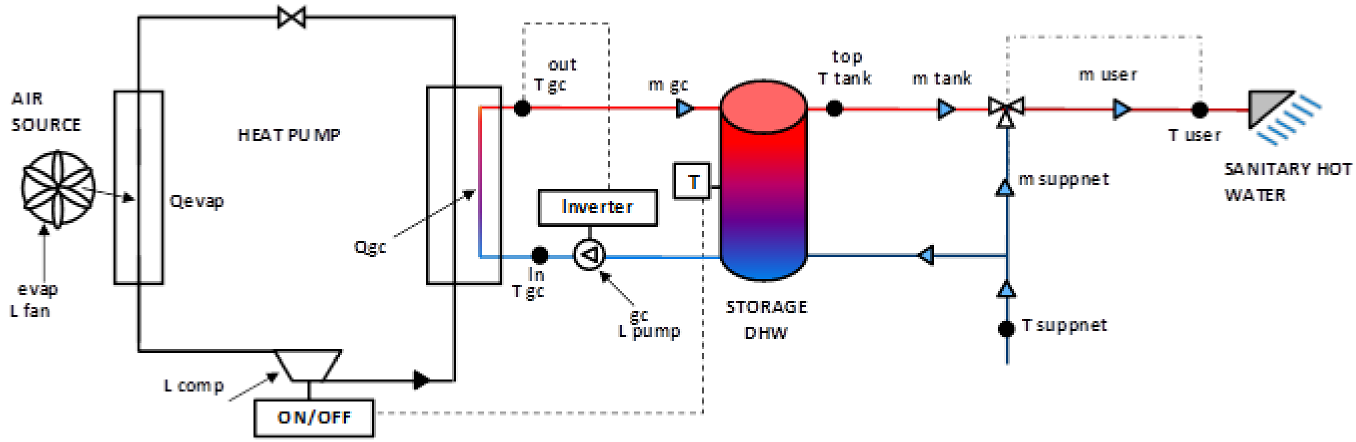

Figure 7. Schematic of the system, reference case control logic.

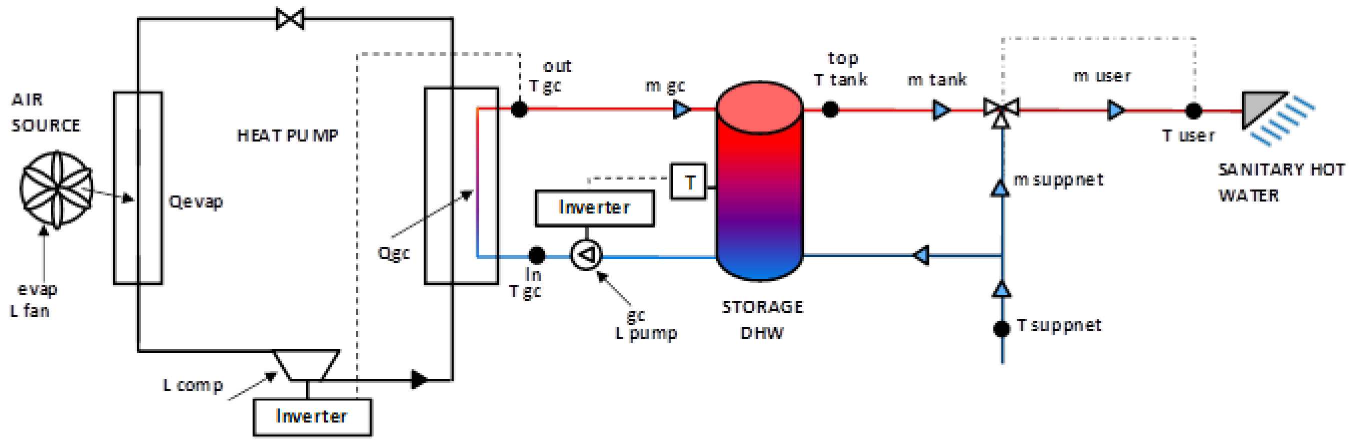

Figure 8. Schematic of the system, inverter case control logic.

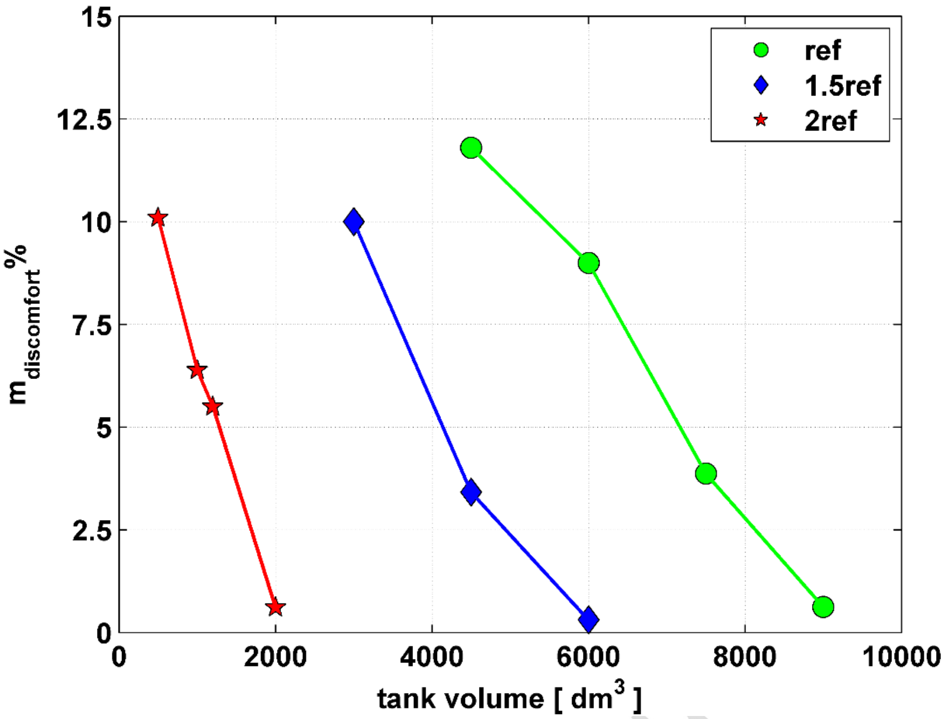

Figure 9. Discomfort as a function of storage size.

a)

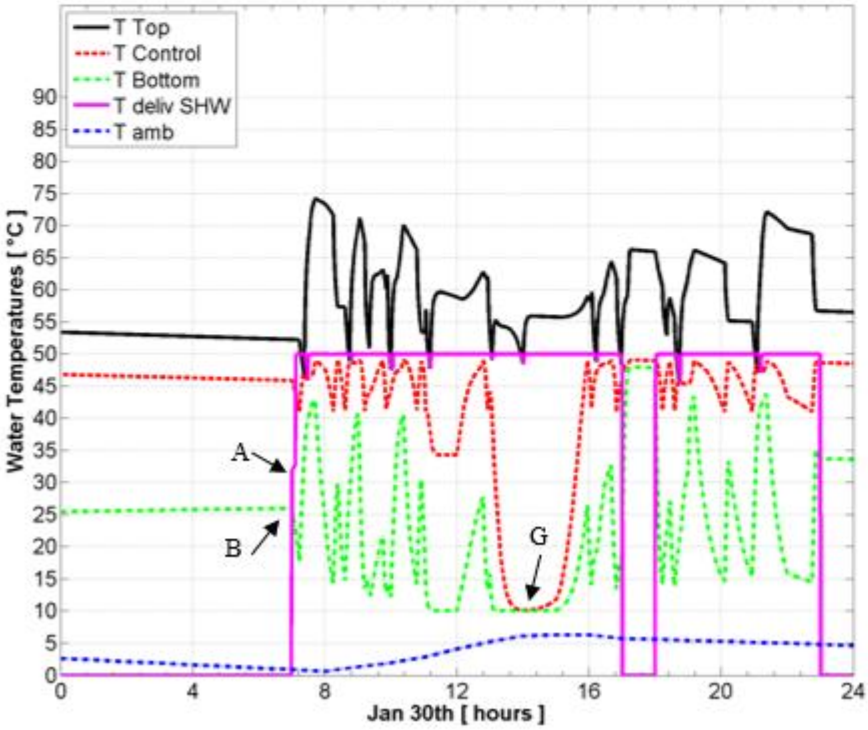

b)

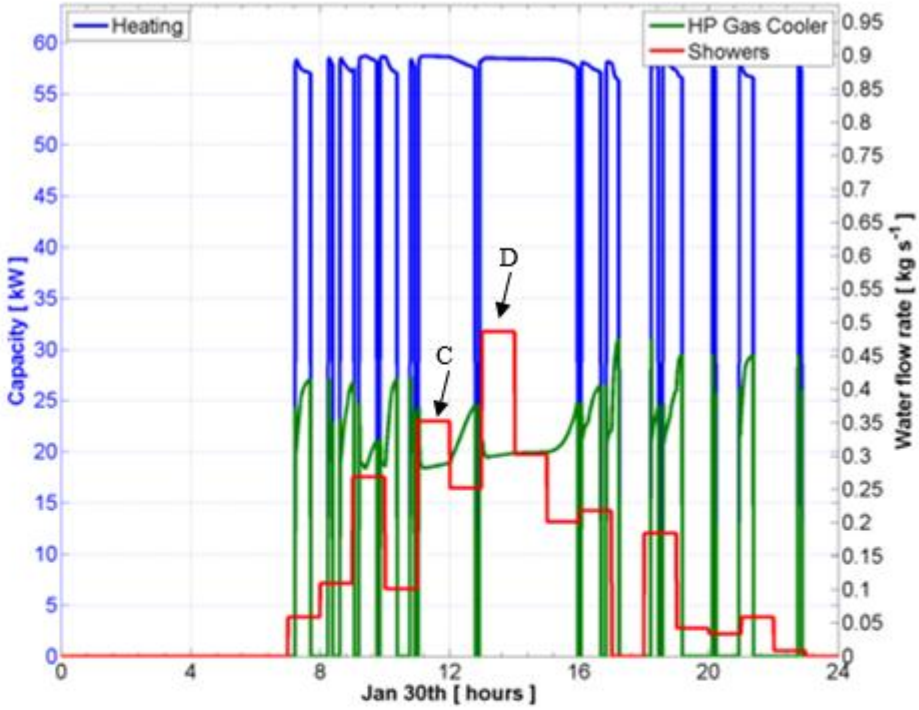

Figure 10a) and 10b). Performance of the system *2ref* during one day, reference control logic.

a)

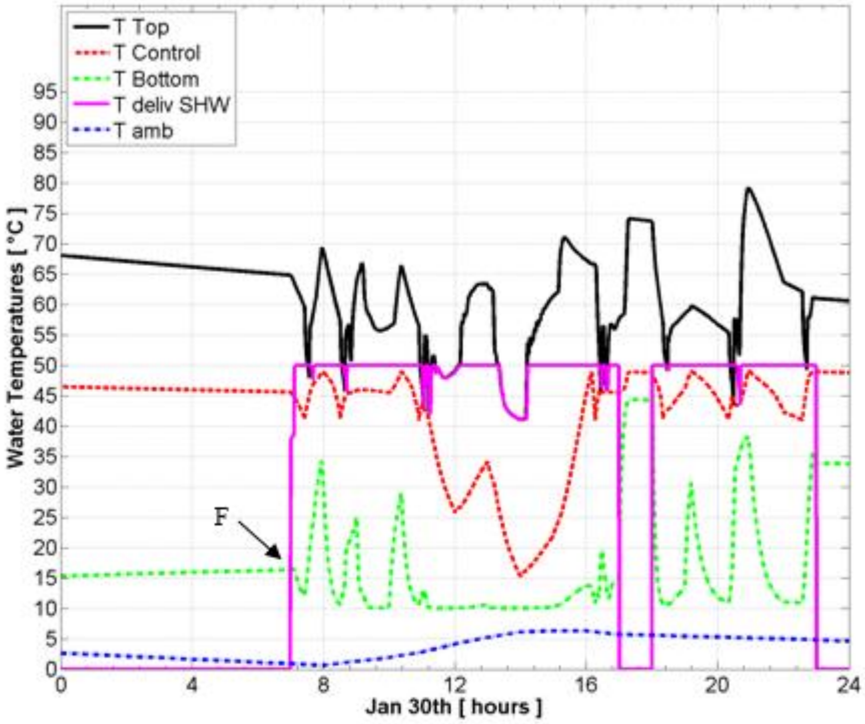

b)

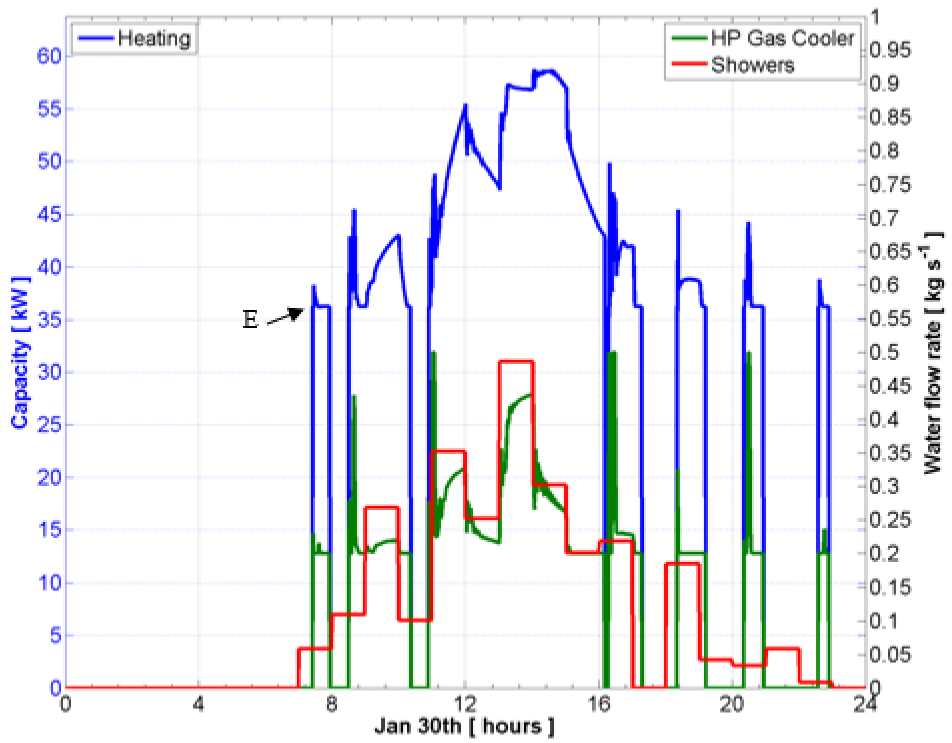

Figure 11a) and 11b). Performance of the system *2ref-inv* during one day, inverter control logic.

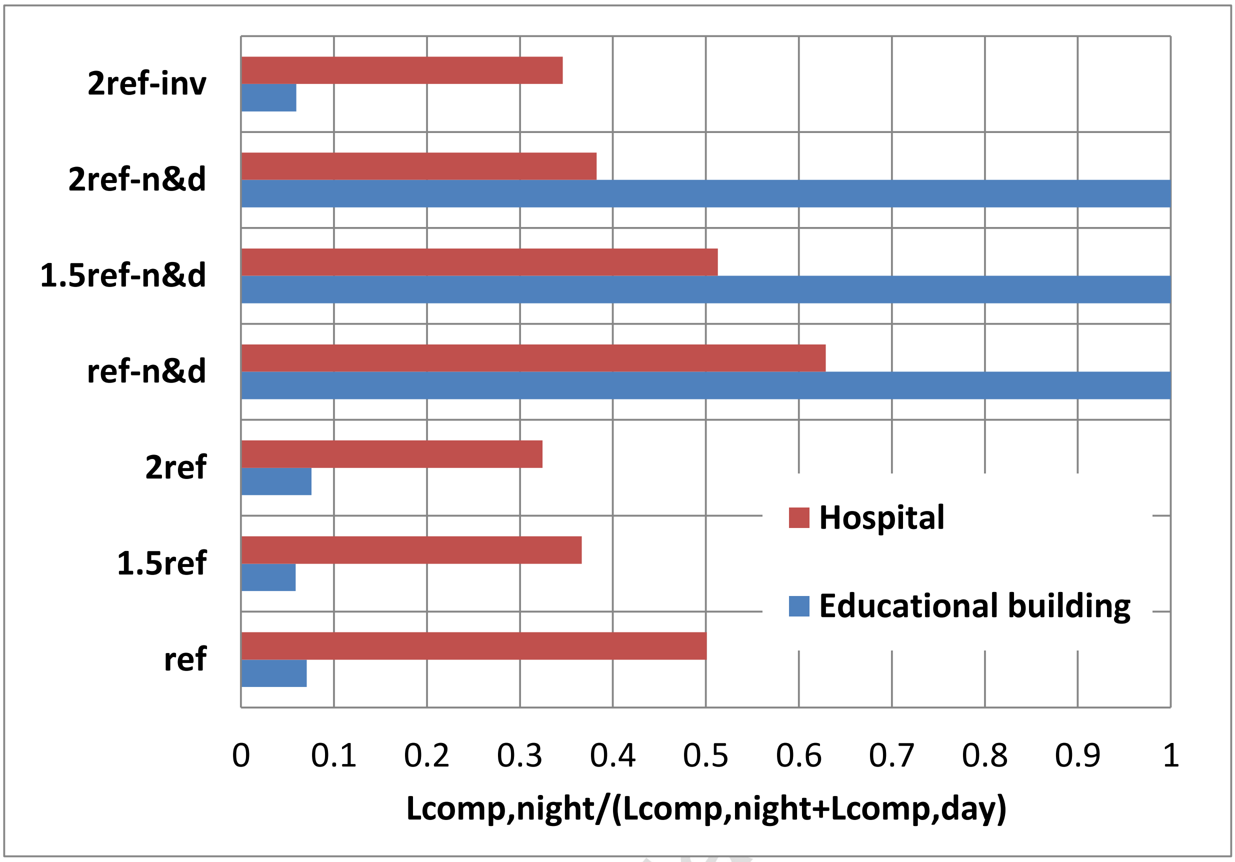

Figure 12. Running costs as a function of the electricity price ratio for the educational building.

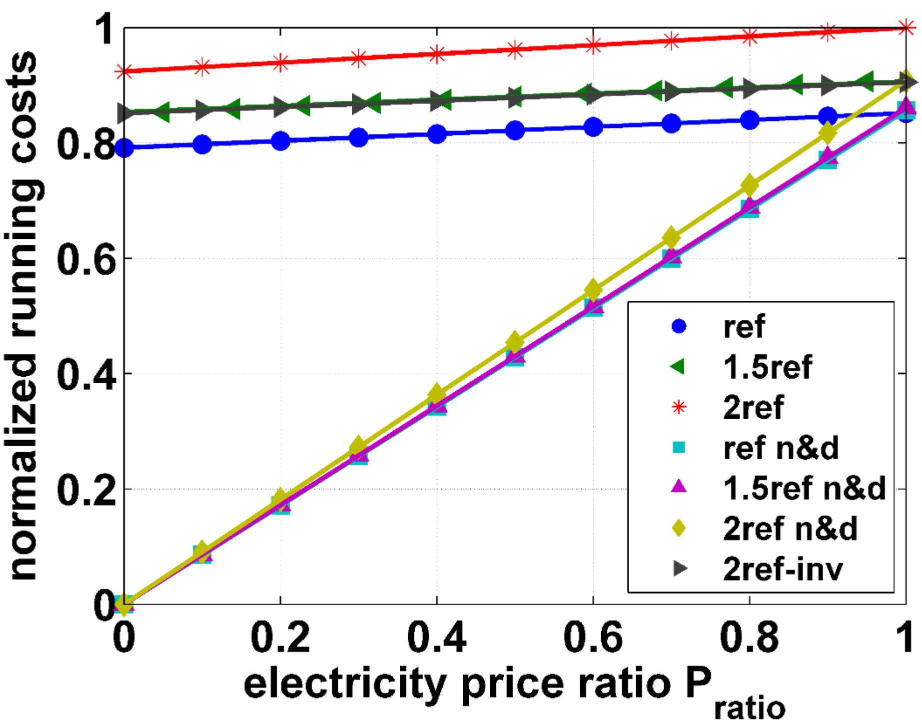

Figure 13. Running costs as a function of the electricity price ratio for the educational building.

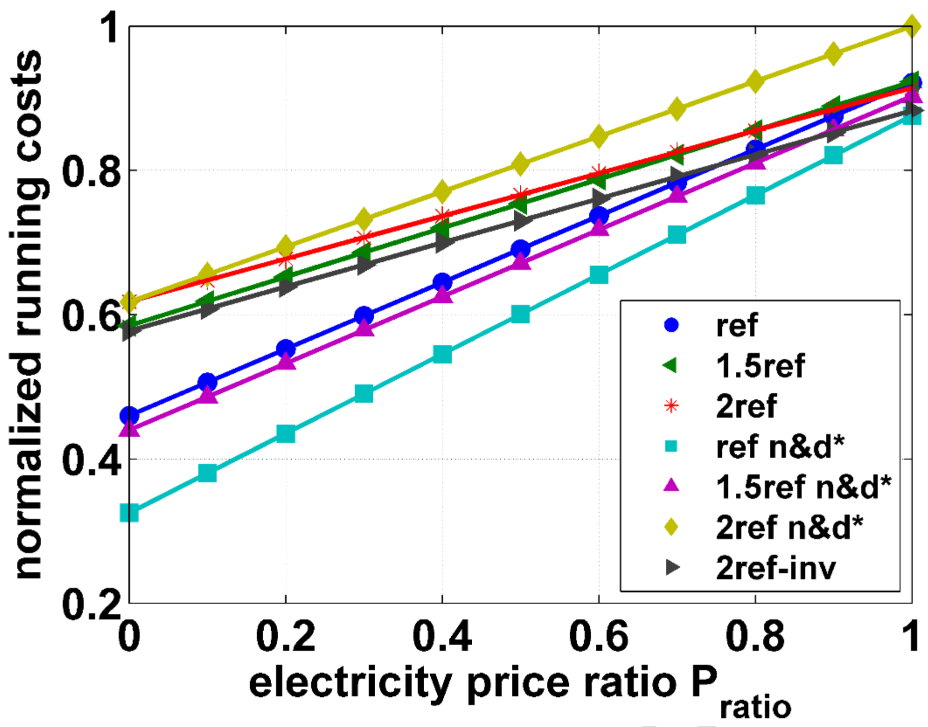

Figure 14. Running costs as a function of the electricity price ratio for the hospital.

TABLES WITH CAPTIONS

Table 1. Coefficients $p_n$of the heat pump correlations.

	p_1	p_2	p_3	p_4
$\dot{Q}_{gc}$	31.07	0.760	-0.256	-0.002
$\dot{L}_{comp}$	8.575	0.106	0.049	-0.004
COP	3.655	0.049	-0.072	0.002

Table 2. Scaling factors and intervals of boundary conditions considered to obtain the correlations.

	$\frac{\dot{V}_{comp}}{V_{comp,ref}}$	$\frac{A_{gc}}{A_{gc,ref}}$	$\frac{A_{ev}}{A_{ev,ref}}$	$\frac{\dot{V}_{fan}}{V_{fan,ref}}$	T_{amb} (from : to)	$T_{in,gc}$ (from : to)	$\dot{m}_{gc}$ (from : to)
					[°C]	[°C]	[kg/h]
ref	1	1	1	1	-10 : 22	10 : 20	320 : 1250
1.5ref	1.5	1.5	1.5	1.5	-10 : 22	10 : 20	320 : 1250
2ref	2	2	2	2	-10 : 22	10 : 20	480 : 1800
inv	1	2	2	2	-10 : 22	10 : 20	320 : 1800

Table 3. Input data to the discomfort vs storage size set of simulations. Reference case control logic.

EHP_{size}	$\dot{m}_{gc}$ (min - max)	V_{tank} (from : to)	$\%V_{hot}$	T_{set}	db
	[kg/h]	[dm^3]	%	[°C]	[°C]
ref	240 - 600	4500 : 9000	50	45	5
1.5ref	360 - 900	3000 : 6000	50	45	5
2ref	480 - 1200	500 : 2000	50	45	5

1 Table 4. Results of the discomfort vs storage size set of simulations. Reference case control logic.

EHP_{size}	V_{tank}	$\% \dot{m}_{discomfort}$	$ON\%$	$SPF1$
	[dm^3]	%	%	
ref	9000	0.63	48.5	4.57
ref	7500	3.87	46.6	4.57
ref	6000	9.00	45.7	4.56
ref	4500	11.8	44.0	4.56
1.5ref	6000	0.31	32.3	4.57
1.5ref	4500	3.42	32.0	4.57
1.5ref	3000	10.0	31.3	4.57
2ref	2000	0.61	25.2	4.74
2ref	1200	5.50	25.3	4.76
2ref	1000	6.39	25.5	4.76
2ref	500	10.1	26.8	4.84

2 Table 5. Input datafor the control logic comparison. Educational building load profile.

EHP_{size}	*control logic*	$\dot{m}_{gc}$ (min - max)	$\%V_{hot}$	T_{set}	db
		[kg/h]	%	[°C]	[°C]
ref	**reference**	240 - 600	80	45	5
1.5ref	**reference**	360 - 900	80	45	5
2ref	**reference**	480 - 1200	80	45	5
ref	**night&day**	240 - 600	80	45	5
1.5ref	**night&day**	360 - 900	80	45	5
2ref	**night&day**	480 - 1200	80	45	5
2ref-inv	**inverter**	480 - 1200	80	45	5

3

Table 6. Results for the control logic comparison. Educational building load profile.

EHP_{size}	control logic	V_{tank} ($\% \dot{m}_{discomfort} \approx 5\%$)	ON	$SPF1$	adc	$T_{bottom,avg}$	$L_{comp,day}$	$L_{comp,night}$
		[dm^3]	%		[h]	[°C]	[kWh]	[kWh]
ref	**reference**	2750	33.7	4.58	5.21	14.1	21783	1653
1.5ref	**reference**	1400	27.4	4.58	1.40	17.2	23487	1462
2ref	**reference**	500	27.4	4.36	0.16	22.8	25425	2088
ref	**night&day**	11400	33.9	4.58	10.46	16.8	0	23558
1.5ref	**night&day**	9800	25.9	4.57	8.12	19.3	0	23682
2ref	**night&day**	8700	21.0	4.34	6.31	17.3	0	24985
2ref-inv	**inverter**	430	32.6	4.61	1.06	16.9	23426	1483

Table 7. Input datafor the control logic comparison. Hospital load profile.

EHP_{size}	control logic	$\dot{m}_{gc}$ (min - max)	$\% V_{hot}$		T_{set}	db
		[kg/h]	%		[°C]	[°C]
ref	**reference**	240 - 600	80		45	5
1.5ref	**reference**	360 - 900	80		45	5
2ref	**reference**	480 - 1200	80		45	5
ref	**night&day***	240 - 600	*20 (day)	*80 (night)	45	5
1.5ref	**night&day***	360 - 900	*20 (day)	*80 (night)	45	5
2ref	**night&day***	480 - 1200	*20 (day)	*80 (night)	45	5
2ref-inv	**inverter**	480 - 1200	80		45	5

Table 8. Results for the control logic comparison. Hospital load profile.

EHP_{size}	*control logic*	V_{tank} $(\%\ \dot{m}_{discomfort} \approx 5\%)$	ON	$SPF1$	adc	$T_{bottom,avg}$	$L_{comp,day}$	$L_{comp,night}$
		[dm^3]	%		[h]	[°C]	[kWh]	[kWh]
ref	**reference**	4600	82.0	4.50	19.68	12.1	29010	29107
1.5ref	**reference**	2200	63.7	4.57	5.74	13.0	36880	21336
2ref	**reference**	1450	56.9	4.41	1.05	17.1	38981	18692
ref	**night&day***	13500	79.4	4.58	19.01	10.4	20502	34731
1.5ref	**night&day***	3800	62.2	4.56	9.71	12.1	27740	29199
2ref	**night&day***	1900	53.1	4.36	2.08	11.7	38948	24118
2ref-inv	**inverter**	1250	66.4	4.63	4.46	12.5	36426	19264